日本シミュレーション学会論文誌，Vol.12, No.1, pp. 2–7, 2020

論 文

Special Section on the JSST2019 Student Session

Numerical Prediction for Damping Effects of Suspended Deformable Bodies on Wave Motions of Free-Surface Flows†

Satoru Ushijima*1, Niku Guinea*2 and Daisuke Toriu*1

Abstract The damping effects on the free-surface motions due to the presence of the deformable solid bodies suspended in the fluid were numerically investigated. The computational method is based on a full Eulerian model that can deal with the interactions between Newtonian fluids and visco-hyperelastic solid bodies. In the numerical predictions, the free-surface motions caused by the so-called dam-break conditions, including four spherical visco-hyperelastic bodies, were calculated with two cases of non-dimensional shear moduli, $G = 0.1$ and 10.0, of the visco-hyperelastic bodies, which have the same density as that of the liquid phase. As a result of the computations, the following reasonable results were obtained; when the solid bodies are highly flexible ($G = 0.1$), the free-surface motions are almost the same as those having no solid bodies. In contrast, it was demonstrated that the damping effects are obviously large in case that the stiffness of solid bodies increases ($G = 10.0$).

Key words Fluid-solid interaction, Visco-hyperelastic material, Free-surface flow, Full Eulerian method, Parallel computation

1. Introduction

It is widely known that the free-surface motions are affected by the solid objects included in the fluid. In many instances actually observed, various efforts have been made to reduce the free-surface wave motions, sloshing and splashing by setting up some solid objects and structures in the flows, since they can cause damages and unfavorable outcomes. Such examples can be found in the rigid and flexible devices employed in storage tanks to suppress slosh dynamics as well as in the breakwaters to prevent large coastal waves due to typhoons and tsunamis.

A lot of numerical studies have been conducted to solve these problems with various computational methods: an Eulerian-Lagrangian method to simulate the interactions between an elastic body and fluids[1)] and floating buoys affected by free-surface motions[2)], a fully Eulerian method for a suspended soft body in cavity flows[3,4)] as well as a fully Lagrangian method for a deformable floating structure in free-surface flows[5)].

In most of the previous studies, however, it is seen that the effects of solid bodies on the free-surface motions were mainly studied without focusing on how the flexibility of the bodies can affect the wave motions. In case that the solid objects are made of highly flexible material and their density is almost the same as that of the fluid, it is expected that the effects on the free-surface motions decrease as the flexibility of the material increases. In the present study, numerical predictions are conducted to demonstrate the effects of deformable solid objects included in the fluids on the wave motions to understand that such tendencies can be treated with numerical simulations.

For this purpose, a fully Eulerian numerical method for visco-hyperelastic solid objects[6,7)] is employed and it is implemented in our computational method, in which a finite volume method (FVM) is used in the collocated grid system[8)]. Since the governing equations for gas, liquid and solid phases can be treated in the Eulerian grid system without tracking individual solid objects, it is easy to adopt a domain decomposition method to parallelize the computations in the distributed memory system.

In this study, the dam-break flows including spherical visco-hyperelastic bodies were calculated to investigate the damping effects of the flexibility of the suspended objects on free-surface motions. Thus, two cases of computations were conducted with non-dimensional shear moduli $G = 0.1$ and 10.0. As a result of the computations, it was demonstrated that the free-surface motions are almost the same as those having no solid bodies when the visco-

*1 Academic Center for Computing and Media Studies (ACCMS), Kyoto University
*2 Research Student, ACCMS, Kyoto University
† 2020 年 1 月 10 日受付・2020 年 3 月 11 日再受付

hyperelastic bodies are highly flexible ($G = 0.1$), while the damping effects are large in case that the stiffness of solid bodies relatively increases ($G = 10.0$).

2. Numerical Methods

2.1 Phase-averaged governing equations

In the present paper, numerical predictions are conducted for the multiphase field, consisting of three phases: gas, liquid and visco-hyperelastic solid phases. In order to deal with such multiple phases in the Eulerian method rather than usual Lagrangian or Eulerian-Lagrangian methods, the governing equations for all phases are averaged in a similar way to the multiphase model proposed by Ushijima et al.[9]. The derived phase-averaged governing equations are able to be discretized in the Eulerian grid system.

The phase-averaged governing equations are derived for the multiphase fields consisting of incompressible gas and liquid in addition to the incompressible visco-hyperelastic solid. In the derivation of the multiphase model, the governing equations are averaged in a fluid cell as shown in **Fig. 1**. The volume fractions of gas, liquid and solid phases in a computational cell are indicated as ϕ_G, ϕ_L and ϕ_S respectively as illustrated in **Fig. 1**. The computational cell is a minimum unit used in FVM as will be explained in detail later on. The volume fractions satisfy the following relationship:

$$\phi_G + \phi_L + \phi_S = 1 \tag{1}$$

Regarding the momentum equations, since the equations with conservative forms are used in the process of phase averaging, the obtained velocity is defined as a mass-averaged velocity. Meanwhile, the other variables are treated as the volume-averaged ones[9].

Firstly, the following incompressible condition establishes due to the assumption of incompressibility of all phases:

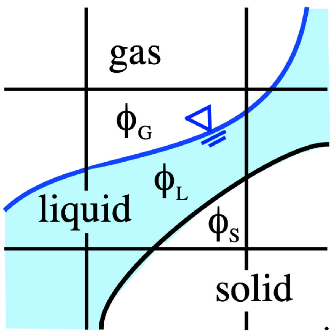

Fig. 1 A computational cell and volume fractions (ϕ_G, ϕ_L and ϕ_S)

$$\frac{\partial u_j}{\partial x_j} = 0 \tag{2}$$

where u_j is the averaged velocity component in x_j direction in three-dimensional Cartesian coordinates. Then, the mass conservation equation is derived as follows:

$$\frac{\partial \rho}{\partial t} + \frac{\partial (\rho u_j)}{\partial x_j} = 0 \tag{3}$$

where t is time and ρ is volume-averaged density. The momentum equations are given by

$$\frac{\partial (\rho u_i)}{\partial t} + \frac{\partial (\rho u_i u_j)}{\partial x_j} = -\frac{\partial p}{\partial x_i} + \frac{\partial (\mu D_{ij})}{\partial x_j} + \frac{\partial (G \phi_S^{\frac{1}{2}} B^{*\prime}_{ij})}{\partial x_j} + \rho f_i \tag{4}$$

where p is pressure, f_i is the external force in x_i direction, μ is the coefficient of viscosity and G is the shear modulus of the hyperelastic material. The form of the third term on the right-hand side of Eq. (4) is determined with reference to the preceding study[6]. In case that the fluid cell does not include solid phase, which means $\phi_S = 0$, the corresponding term is neglected and Eq. (4) turns to be a usual Navier-Stokes equation.

In Eq. (4), D_{ij} is the component of the deformation rate tensor defined by

$$D_{ij} = \frac{\partial u_i}{\partial x_j} + \frac{\partial u_j}{\partial x_i} \tag{5}$$

In addition, B_{ij} is a component of the left Cauchy-Green deformation tensor B, while $B^*{}_{ij}$ is the component of its deviation tensor given by

$$B^*{}_{ij} = B_{ij} - \frac{1}{3}\mathrm{tr}(B)\delta_{ij} \tag{6}$$

where $\mathrm{tr}(B)$ is the trace of tensor B and δ_{ij} is the Kronecker's delta. The tensor component $B^{*\prime}_{ij}$ in Eq. (4) is defined with reference to the preceding study[6] as follows:

$$B^{*\prime}_{ij} = \phi_S^{1/2} B^*_{ij} \tag{7}$$

In order to determine the $B^*{}_{ij}$ in Eq. (7), the following governing equations are used

$$\frac{\partial B^*_{ij}}{\partial t} + \frac{\partial (B^*_{ij} u_k)}{\partial x_k} = L_{ik} B^*_{kj} + B^*_{ik} L_{kj} \tag{8}$$

where L_{ij} is a component of velocity gradient tensor given by $L_{ij} = \partial u_i / \partial x_j$.

Finally, the convection equations for ϕ_L and ϕ_S with conservative forms are given by

$$\frac{\partial \phi_L}{\partial t} + \frac{\partial(\phi_L u_j)}{\partial x_j} = 0 \tag{9}$$

and

$$\frac{\partial \phi_S}{\partial t} + \frac{\partial(\phi_S u_j)}{\partial x_j} = 0 \tag{10}$$

The remaining volume fraction ϕ_G can be estimated as $\phi_G = 1 - \phi_L - \phi_S$.

2.2 Numerical procedures

Figure 2 shows a schematic view of the whole computational area including three phases with the computational cells and the subdomains. The scale of the computational cell is set up finer than the solid object. The computational domain is decomposed into multiple subdomains as shown in **Fig. 2**, so that the computations of the discretized governing equations can be parallelized with message passing interface (MPI) [10] in the distributed memory system. Compared with the computational methods in which solid objects are treated in a Lagrangian way, the present Eulerian method enables us to easily parallelize the computations of the movements of the solid objects, since individual solid objects need not to be tracked among subdomains.

The governing equations shown in the above subsection are discretized with FVM in the three-dimensional collocated grid system[8]. A computational cell in the collocated grid system is shown in **Fig. 3**.

The discretized variables are located at the cell center point C as well as the cell boundaries indicated by B in **Fig. 3**. The velocity components u_{ci} at cell center points are spatially interpolated to obtain u_{bi} defined on the cell boundaries. In a way similar to the computational method[8] based on FVM, the convection and diffusion equations are implicitly calculated at the center point of each cell using the estimated fluxes on the cell boundaries. In particular, the fluxes for the convection terms are calculated with the 5th-order TVD scheme[11]. In particular, the interpolated u_{ci} is used to calculate pressure-Poisson equations to satisfy incompressible condition on the basis of the C-HSMAC method[12] in order to avoid so-called pressure-velocity coupling oscillations.

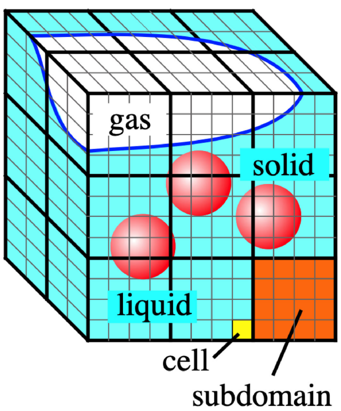

Fig. 2　Schematic view of computational domain

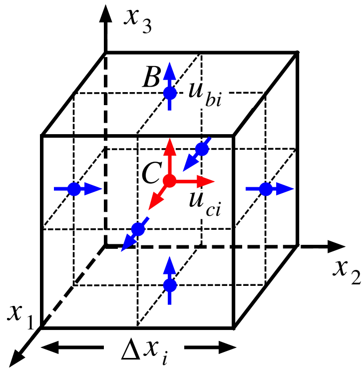

Fig. 3　Computational cell in collocated grid system

3. Application of Computational Method

3.1 Conditions of numerical experiments

The present computational method was applied to the dam-break flows including four deformable spheres as illustrated in **Fig. 4**. All variables in computations are non-dimensionalized with representative values.

The lengths of the computational region in **Fig. 4** are $L_1 = 2.1$, $L_2 = 1.0$ and $L_3 = 1.0$ in x_1, x_2 and x_3 directions, respectively. The initial liquid depths of the dam-break

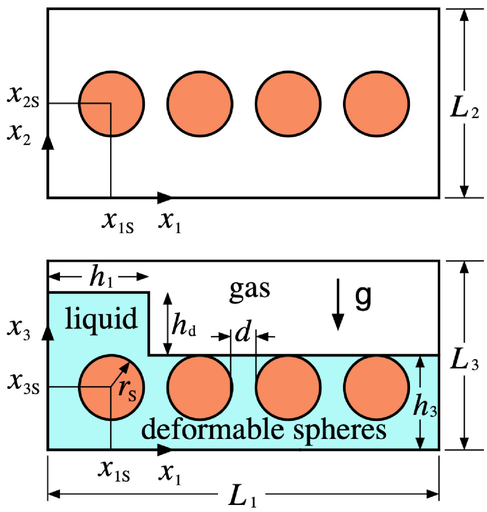

Fig. 4　Computational area with initial free-surface profile and solid spheres (top = plan view, bottom = side view)

condition are 0.8 ($x_1 \leq 0.25L_1$) and 0.5 ($x_1 > 0.25L_1$), which means $h_1 = 0.25L_1$, $h_d = 0.3$ and $h_3 = 0.5$ shown in **Fig. 4**. The gravitational acceleration g is -10.0 acting in x_3 direction.

In the initial conditions shown in **Fig. 4**, the initial radius r_s of the spherical visco-hyperelastic bodies is 0.2 and the interval of the center points of the neighboring two spheres is 0.5, which means $d = 0.1$ in **Fig. 4**. The initial center point of the sphere located on the leftmost side is set at $(x_{1S}, x_{2S}, x_{3S}) = (0.3, 0.5, 0.3)$.

On all boundaries, the pressure boundary conditions are $\partial p/\partial n = 0$, while non-slip conditions are used for velocity except on the top wall where the free-slip condition is adopted. The densities of the gas and liquid are 1.0 and 1.0×10^3 respectively, while the viscous coefficients of the gas and liquid phases are set at 1.0×10^{-2}. Similarly, the viscous coefficient of the visco-hyperelastic body is also 1.0×10^{-2}. The density of visco-hyperelastic bodies is 1.0×10^3, which is the same as that of the liquid phase. Thus, four visco-hyperelastic bodies are suspended in the liquid.

The computational domain was decomposed into $6 \times 1 \times 2$ subdomains in x_1, x_2 and x_3 directions, respectively. The parallel computations were conducted with 12 cores of the Intel Xeon Broadwell (2.1 GHz). The elapsed computational time was about 1 hour to calculate 5,000 steps which correspond to $t = 5.0$.

In order to investigate the relationships between the wave motions of the free-surface and the stiffness of the deformable bodies, two cases of computations were conducted; shear moduli are set at $G = 10.0$ and $G = 0.1$. The computational results of free-surface profiles and the shapes of the spheres are visualized, while the free-surface levels are quantitatively compared between two cases with reference to the dam-break flow without spheres.

3.2 Results and discussion

Figure 5 shows the free-surface profiles and the shapes of the four visco-hyperelastic bodies with $G = 10.0$, while **Fig. 6** shows the results with $G = 0.1$. Comparing two results having different G, it can be seen that the initial spherical shapes are almost unchanged in case that $G = 10.0$ and that they are largely deformed due to the interactions with the free-surface flows in case that $G = 0.1$.

In order to compare the wave motions in the two results having different G, the time histories of the liquid levels h_L on the left wall (on the $x_1 = 0$ section) are shown in **Fig. 7** as well as the results calculated without solid bodies in the flow. Comparing with the h_L obtained without solid bodies,

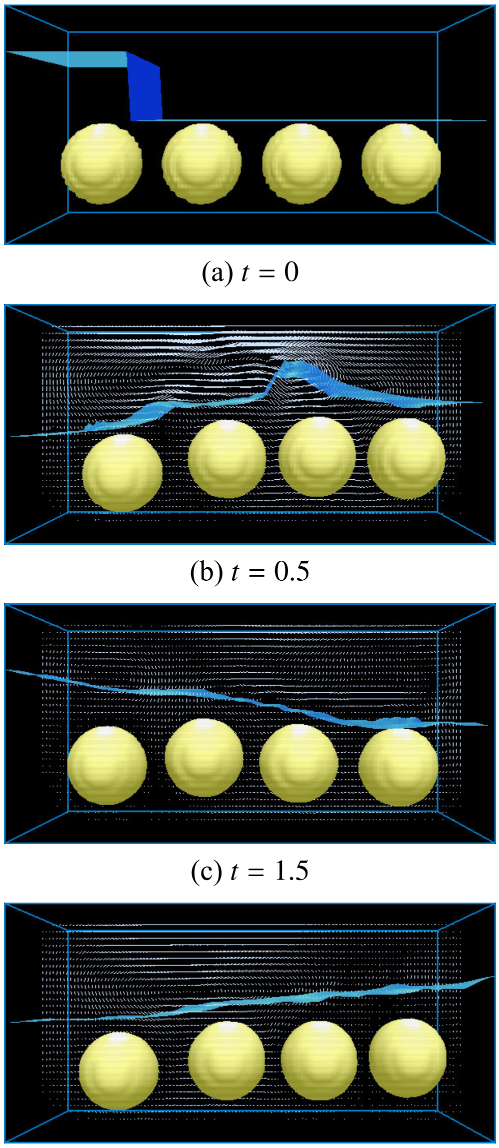

(a) $t = 0$ (b) $t = 0.5$ (c) $t = 1.5$ (d) $t = 2.0$

Fig. 5 Free surfaces and deformable bodies ($G = 10.0$)

the amplitudes of the liquid levels h_L are largely decreased when $G = 10.0$ as shown in **Fig. 7** (a), while the damping effects are scarcely found in case that $G = 0.1$ in **Fig. 7** (b). It can be thought reasonable that the damping effects on the free-surface motions generally increase as the stiffness of the deformable bodies increases. Conclusively, it can be seen that such tendencies are successfully demonstrated with the present computational results.

4. Conclusions

In this study, the damping effects of the suspended deformable bodies on the free-surface motions were numerically investigated. The computational method is based on the full Eulerian method that can deal with the

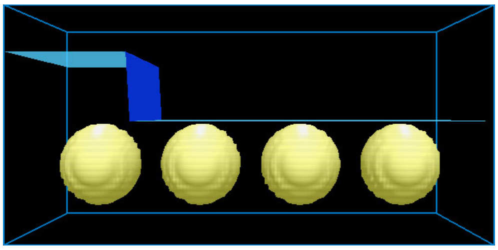

(a) $t = 0$

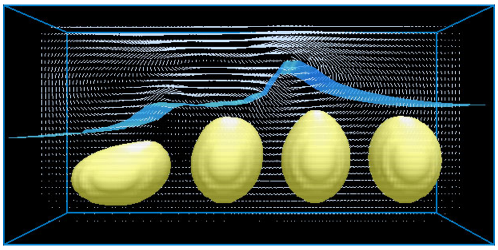

(b) $t = 0.5$

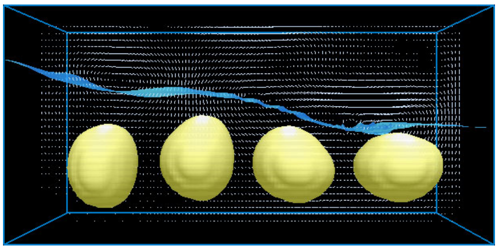

(c) $t = 1.5$

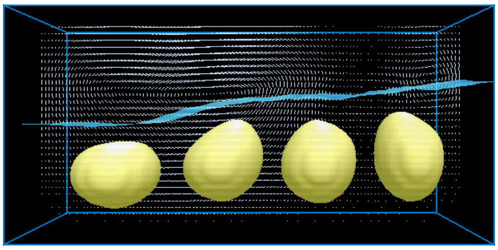

(d) $t = 2.0$

Fig. 6　Free surfaces and deformable bodies ($G = 0.1$)

interactions between the Newtonian fluids and visco-hyperelastic solid bodies. Thus, all phases, consisting of gas, liquid and solid, are treated in the Eulerian collocated grid system. This computational method has some advantages; it is easy to apply the domain decomposition method to parallelize the numerical procedures and individual solid bodies need not be tracked among the subdomains, differently from the Lagrangian treatments for solid objects.

In the numerical predictions, the free-surface motions caused by the dam-break conditions, including four spherical visco-hyperelastic bodies, were calculated with two cases of non-dimensional shear moduli, $G = 0.1$ and 10.0, of the visco-hyperelastic bodies, which have the same density as that of the liquid. As a result of the computations, it is shown that the following reasonable results were obtained; when the solid bodies are highly flexible ($G = 0.1$), the free-surface motions are almost the same as those having no solid bodies. In contrast, it was demonstrated that the damping effects are obviously large in case that the solid bodies are relatively rigid ($G = 10.0$), in which the deformations of solid bodies are relatively small.

It is expected that the present computational method allows us to predict the free-surface motions in the flows, including many deformable solid bodies suspended in the liquid and fixed on boundaries as well, in various engineering equipment, such as storage tanks, in addition to the natural hydraulics problems in the waves arising in near-shore regions. Furthermore, the present method possibly enables us to estimate the transportation of many deformable bodies in the flow with and without free-surfaces in the bio-engineering problems and the other various engineering fields.

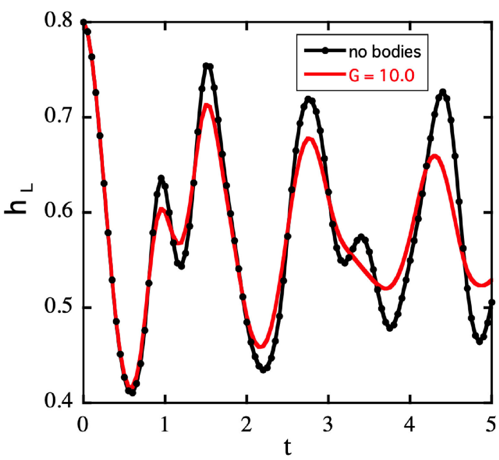

(a) $G = 10.0$

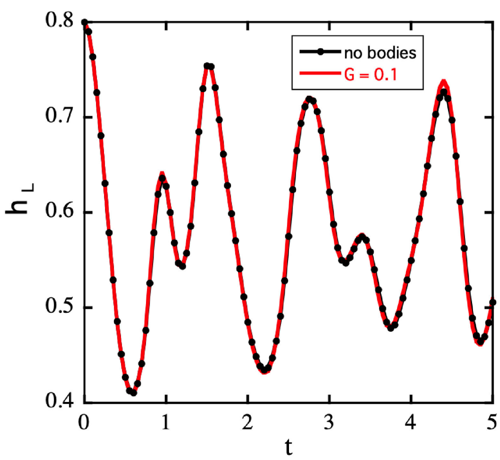

(b) $G = 0.1$

Fig. 7　Comparisons of time histories of h_L with and without deformable bodies

References

1) P. J. Martnez-Ferrer, L. Qian, Z. Ma, D. M. Causon and C. G. Mingham: An efficient finite-volume method to study the interaction of two-phase fluid flows with elastic structures, Journal of Fluids and Structures, **83**, 54/71 (2018)
2) Q. Chen, J. Zang, D. Ning, C. Blenkinsopp and J. Gao: A 3d parallel particle-in-cell solver for extreme wave interaction with floating bodies, Ocean Engineering, **179**, 1/12 (2019)
3) K. Sugiyama, S. Ii, K. Shimizu, S. Noda and S. Takagi: A full eulerian method for fluid-structure interaction problems, Procedia IUTAM, **20**, 159/166, 24th International Congress of Theoretical and Applied Mechanics (2017)
4) S. S. Jain, K. Kamrin and A. Mani: A conservative and non-dissipative eulerian formulation for the simulation of soft solids in fluids, Journal of Computational Physics, **399**, 108922 (2019)
5) Y. Sun, G. Xi and Z. Sun: A fully lagrangian method for fluidstructure interaction problems with deformable floating structure, Journal of Fluids and Structures, **90**, 379/395 (2019)
6) K. Sugiyama, S. Ii, S. Takeuchi, S. Takagi and Y. Matsumoto: A full eulerian finite difference approach for solving fluid-structure coupling problems, Journal of Computational Physics, **230**-3, 596/627 (2011)
7) K. Nishiguchi, K. Maeda, S. Okazawa and S. Tanaka: A visco-hyperelastic analysis scheme by using a full eulerian finite element method for dynamics of pressure-sensitive adhesives, Transactions of the Japan Society of Mechanical Engineers, Series A, **78**-788, 375/389 (2012)
8) S. Ushijima, Y. Okuyama and I. Nezu: Implicit computational algorithm for 3D incompressible flows with collocated grid system and its parallelization, J. Applied Mech. JSCE, **6**, 185/192 (2003)
9) S. Ushijima, A. Fukutani and O. Makino: Prediction method for movements with collisions of arbitrarily-shaped objects in 3D free-surface flows, JSCE Journal, **64**/II-2, 128–138 (2008) (in Japanese)
10) W. Gropp, E. Lusk and R. Thakur: Using MPI-2, The MIT Press (1999)
11) S. Yamamoto and H. Daiguji: Higher-order-accurate upwind schemes for solving the compressible Euler and Navier-Stokes equations, Computers & Fluids, **22**-2/3, 259/270 (1993)
12) S. Ushijima, H. Tanaka and D. Toriu: Validity of pressure-velocity correction algorithm (C-HSMAC method) for incompressible fluids with passive scalar convection, J. Adv. Simulat. Sci. Eng., **6**-1, 260/272 (2019)

Author Inforamtion

Satoru Ushijima

He graduated from faculty of engineering of Kyoto University in 1982 and received Master's degree in 1984 from Kyoto University. He received Dr. Eng. from Kyoto University in 1990. He is currently a professor in ACCMS (Academic Center of Computing and Media Studies) in Kyoto University.

Niku Guinea

He graduated from faculty of civil and environment engineering of Institut Teknologi Bandung, Indonesia majoring in Ocean Engineering program in 2016 He is currently a research student in ACCMS (Academic Center of Computing and Media Studies) in Kyoto University.

Daisuke Toriu

He graduated from faculty of engineering of Kyoto University in 2011 and received Master's degree in 2013 from Kyoto University. He received Dr. Eng. from Kyoto University in 2015. He is currently an assistant professor in ACCMS (Academic Center of Computing and Media Studies) in Kyoto University.